Journal of Macromolecular Science, Part A
Publication details, including instructions for authors and subscription information:
http://www.informaworld.com/smpp/title~content=t713597274

Synthesis, Characterization and Electrorheological Properties of Polyindene/Kaolinite Composites

Cigdem Eristi[a]; Mustafa Yavuz[b]; Hasim Yilmaz[c]; Bekir Sari[a]; Halil Ibrahim Unal[a]
[a] Science Faculty, Chemistry Department, Gazi University, Ankara, Turkey [b] Science Faculty, Chemistry Department, Suleyman Demirel University, Isparta, Turkey [c] Science Faculty, Chemistry Department, Harran University, Sanliurfa, Turkey

To cite this Article Eristi, Cigdem , Yavuz, Mustafa , Yilmaz, Hasim , Sari, Bekir and Unal, Halil Ibrahim(2007) 'Synthesis, Characterization and Electrorheological Properties of Polyindene/Kaolinite Composites', Journal of Macromolecular Science, Part A, 44: 7, 759 — 767
To link to this Article: DOI: 10.1080/10601320701353553
URL: http://dx.doi.org/10.1080/10601320701353553

Journal of Macromolecular Science®, Part A: Pure and Applied Chemistry (2007) **44**, 759–767

ISSN: 1060-1325 print/1520-5738 online
DOI: 10.1080/10601320701353553

Synthesis, Characterization and Electrorheological Properties of Polyindene/Kaolinite Composites

CIGDEM ERISTI,[1] MUSTAFA YAVUZ,[2] HASIM YILMAZ,[3] BEKIR SARI,[1] and HALIL IBRAHIM UNAL[1]

[1]*Science Faculty, Chemistry Department, Gazi University, Ankara, Turkey*
[2]*Science Faculty, Chemistry Department, Suleyman Demirel University, Isparta, Turkey*
[3]*Science Faculty, Chemistry Department, Harran University, Sanliurfa, Turkey*

Received December, 2006, Accepted January, 2007

In this study, synthesis, characterization and electrorheological (ER) properties of polyindene (PIN) and polyindene/kaolinite composites were carried out by cationic radical polymerization using $FeCl_3$ as the oxidizing agent. The homopolymer and composites, containing different amounts of PIN were characterized by FTIR spectroscopy, thermo-gravimetric (TGA) analyses, scanning electron microscopy (SEM) and dynamic light scattering (DLS) methods. The conductivity and dielectric properties of PIN and PIN/kaolinite composites were determined. Suspensions of PIN and PIN/kaolinite composites were prepared in silicone oil (SO), at a series of concentrations ($c = 5–25$ m/m %). The effects of concentration, shear rate, electric field strength, frequency, temperature and promoter on ER activities of suspensions were investigated.

Keywords: polyindene; polyindene/kaolinite conducting composites; electrorheological fluids

1 Introduction

An electrorheological (ER) fluid is typically a suspension of a solid (conductive or polarizable particle) or liquid material (liquid crystal) dispersed in an insulating oil. The increase in the viscosity of suspensions upon application of an electric field is commonly known as ER effect or Winslow effect (1). The rheological properties (i.e., viscosity, shear stress) of an ER suspension can be reversibly changed by several orders of magnitude under an externally applied electric field of several kV/mm. The mechanical properties can be easily controlled within a wide range of almost from a pure liquid to a solid like structure. The ER fluid can be used as an electrical and mechanical media in various industrial areas. Their wide potential application areas stimulated great deal of interests both from academic researchers and industry (2). ER fluids have been considered for various applications in mechanical engineering such as engine mouth, clutches, shock absorber, ER valves, robotic arms and several control systems (3). Recently, ER fluids have found some newly developed applications, such as human muscle stimulators, spacecraft deployment dampers, seismic controlling frame structures, ER tactile displays, and photonic crystals (3). ER fluids are also used as a proton exchange membrane at fuel cells (4).

A wide variety of particulate materials have been selected to prepare ER suspensions. They are zeolite (5), silica (6), chitosan (7), phosphate cellulose (8), carboneous particle (9) and poly(p-phenylene) conducting polymer (10). These materials have been tested as anhydrous ER fluid particles. On the other hand, the continuous phase including silicone or hydrocarbon oils possesses low conductivity and large dielectric breakdown strength. The well-known electrostatic polarization model incorporates the field-induced polarization of the dispersed phase particles relative to the continuous phase, in which the driving force of the particle fibrillation originates mainly from the electrostatic interaction among the particles (11). In addition, it plays a crucial role on the dielectric mismatch between the dispersed and continuous phase, which causes this interaction (2, 12). Although, from an industrial point of view, dry ER suspensions are preferred for industrial applications, there are some suspensions which require additives such as surfactants or polar liquids (promoter) which are called wet (hydrous) ER fluids (13).

Clay minerals have recently been introduced into the field of composites because of their small particle size and intercalation properties, especially in the application of reinforcement of materials with polymers (14, 15, 16).

In this research, polyindene and polyindene/kaolinite conducting composites, as a novel organic dispersed phase, were

Address correspondence to: Halil Ibrahim Unal, Gazi University, Science Faculty, Chemistry Department, Ankara, Turkey. Fax: +90 312 212 22 79; E-mail: hiunal@gazi.edu.tr

synthesized; characterized by several techniques, their suspensions are prepared in silicone oil (SO) and ER properties were investigated.

2 Experimental

Silicone oil, (SO), ($\rho = 0.963$ g/cm^3, $\eta = 2000$ mPas, $\varepsilon = 2.61$, Aldrich, Germany) was used after drying at 130°C for 3 h in a vacuum oven to remove any moisture present.

Indene (Acros Organics, Belgium) was distilled in vacuum (15 mm Hg) prior to use.

The physical properties of kaolinite (kindly provided by Omya Mining Co. Istanbul) are given below:

Chemical formula: $Al_2Si_2O_5(OH)_4$; class: silicate; color: white, density: 2.6 gcm^{-3}, refractive index: 1.55, hardness (Mohs): 2.5, average diameter (d_{50}): 4.8 μm.

Chemical composition: Al_2O_3: >15%, SiO_2: <76%, Fe_2O_3: <0.5%.

Kaolinite was chosen as a clay material to prepare a composite with polyindene, because it is a ubiquitous mineral in sediment systems, cheap and easy to obtain (17).

All the other chemicals were Aldrich products with analytical grade and used as received.

2.1 Synthesis of Polyindene

2.56×10^{-3} mol $FeCl_3$ was dissolved in 60 mL of chloroform. This solution was kept under vigorous magnetic stirring. The reaction temperature was maintained at 20°C under N_2. 8.52×10^{-3} moles of indene were added dropwise into this solution. After carrying out the polymerization reaction for 3 h, polyindene was recovered and washed several times with distilled water and diethyl ether, respectively, to obtain a colorless solution. Finally, the polyindene was dried in vacuum oven at 70°C for 24 h. The synthesis mechanism of indene is given in Scheme 1.

2.2 Synthesis of Polyindene/Kaolinite Composites

First, a certain amount (2.25 g) of kaolinite was introduced into a three-necked round bottom flask. In a separate flask, 2.56×10^{-3} moles of $FeCl_3$ were dissolved in 60 mL of chloroform, keeping the ratio of $FeCl_3$:indene as 3:1. This solution was added into the first flask. The mixture was kept stirring at 20°C under N_2 for 20 min. Indene (0.011 mol) was added into this solution dropwise under N_2. The composite formation reaction was carried out for 3 h. Then the reaction was stopped and the product was recovered. The crude composite product was washed with distilled water and diethyl ether as described earlier. Finally, the pure composite was dried in a vacuum oven at 70°C for 24 h. Five polyindene/kaolinite composites, with various percentages of polyindene were prepared by changing the clay to monomer ratio, and they were coded as follows: 22% PIN/78% kaolinite (K1), 37% PIN/63% kaolinite (K2), 53% PIN/47% kaolinite (K3); 75% PIN/25% kaolinite (K4) and 85% PIN/15% kaolinite (K5).

2.3 Characterization

FTIR spectra of kaolinite, PIN and PIN/kaolinite composite were recorded on a Mattson Model 1000 instrument (UK) as KBr discs.

Scanning electron micrographs of the samples were recorded using a Jeol JSM-6360 LV scanning electron microscope (Japan).

Thermal analysis of PIN and PIN/kaolinite composites were taken on V2.2A Dupont Model 9900 thermo gravimetric analyzer (Raleigh, NC).

Conductivity and dielectric constants of the samples were measured with an HP 4192 A 6F Impedance Analyzer (UK). The current-potential measurements were performed on samples as solid discs (20 mm long, 5 mm wide and 1 mm thick) with a Keithly 220 programmable current source and a Keithly 199 digital multimeter (Ohio) at ambient temperature. The capacitance, C, of ER particles was measured with an HP 4192 A LF impedance analyzer at frequency of 1 MHz at constant temperature (20.0 ± 0.1°C).

Particle size of the samples was determined using a Malvern Mastersizer E, version 1.2b particle size analyzer (UK). During the particle size measurements, samples were dispersed in ethanol and stirred at a constant temperature of 20°C. The data collected were evaluated according to Fraunhofer diffraction theory by the Malvern Software computer (18).

2.4 Preparation of Suspensions

Suspensions from PIN and PIN/kaolinite particles were prepared in silicone oil (SO) at a series of concentrations (c = 5–25 m/m, %), by dispersing definite amount of dispersed phase in calculated amount of continuous phase according to the formula:

$$(\text{m/m, \%}) = [m_{\text{dispersed phase}}/m_{\text{dispersed phase}} + m_{\text{oil}}]. \quad (1)$$

2.5 Electrorheological Measurements

Electrorheological properties of the suspensions were determined with a Termo-Haake RS600 parallel plate electrorheometer (Germany). The gap between the parallel plates was 1.0 mm and the diameters of the upper and lower plates were 35 mm. All experiments were carried out at various temperatures (0–125°C, with 25°C increments.). The potential used in these experiments was also supplied by a 0–12.5 kV (with 0.5 kV increments) dc electric field generator (Fug Electronics, HCL 14, Germany), which enabled resistivitiy to be created during the experiments.

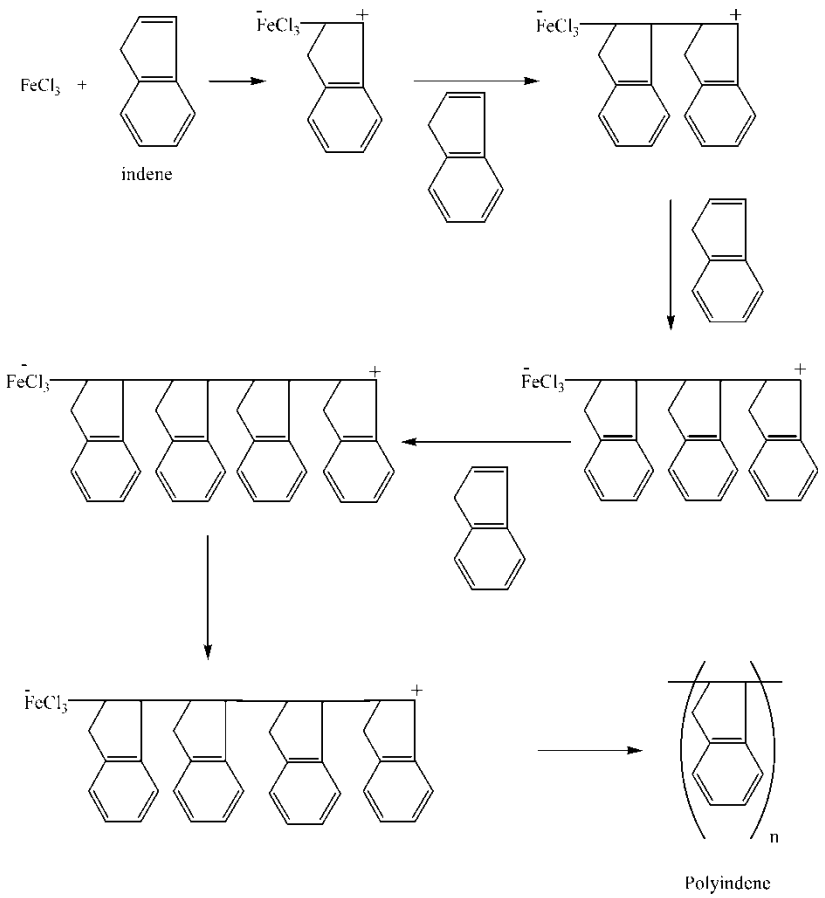

Sch. 1. Polymerization mechanism of indene.

3 Results and Discussions

3.1 Characterization

Characterization of the kaolinite, polyindene and polyindene/kaolinite composites is discussed below:

Table 1 shows the yield percentage, average particle diameter, conductivity and dielectric constant values of PIN and PIN/kaolinite composites. It was observed that, the conductivity and dielectric constant values of PIN and PIN/kaolinite composites are close to each other. The conductivities and dielectric constants of PIN/kaolinite composites slightly increased with increasing content of PIN and they caused no problems during the ER measurements. Similar trends were reported for polyaniline/polyurethane blends by Chwang et al. (19).

FTIR spectra of kaolinite, PIN and PIN/kaolinite composite are given in Figures 1a–c. The FTIR absorptions of kaolinite (Figure 1a) at 3500 cm^{-1}, 3520 cm^{-1}, 3620 cm^{-1} and 3698 cm^{-1} were assigned to the inner hydroxyl group stretchings. FTIR spectrum of PIN (Figure 1b) showed the expected distinctive absorptions: 2920–3000 cm^{-1} (aliphatic C-H stretching), 3020–3037 cm^{-1} (aromatic C-H stretching), 1450–1700 cm^{-1} (aromatic C=C vibrations), 750 cm^{-1} (C-H bending vibrations) (20, 21). The FTIR spectrum of

Table 1. Yield percentage, average particle diameter, conductivity and dielectric constant values of PIN and PIN/kaolinite composites

Composite ratio	Yield (%)	Average particle diameter (μm)	Conductivity $Sm^{-1} \times 10^3$	Dielectric constant
PIN	98	8.29	1.30	12.7
%22 PIN/%78Kaolin (K1)	94	8.94	1.20	10.6
%37 PIN/%63 Kaolin (K2)	94	9.03	1.25	11.0
%53 PIN/%47 Kaolin (K3)	91	12.30	1.36	12.0
%75 PIN/%25 Kaolin (K4)	86	13.15	1.40	12.4
%85 PIN/%15Kaolin (K5)	81	9.21	1.42	12.6

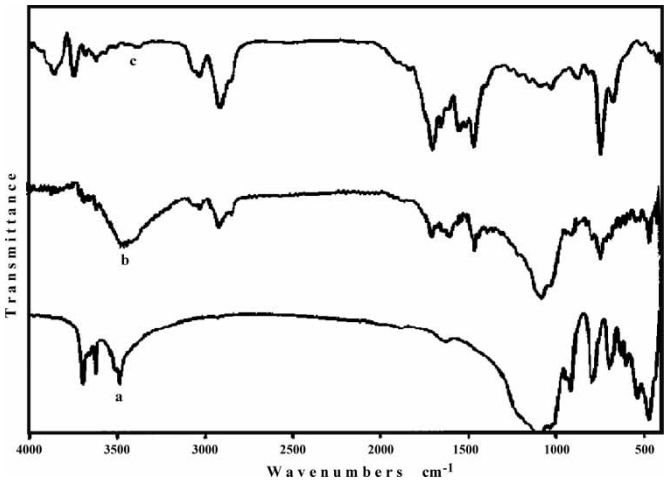

Fig. 1. FTIR spectra of (a) kaolinite, (b) PIN and (c) PIN/kaolinite (K4) composite.

PIN/kaolinite composite (Figure 1c) at 3690 cm^{-1}, 1606 cm^{-1}, and 2922−3023 cm^{-1} are typical of -OH, -C═C- and -C-H stretching vibrations, respectively. The -OH stretching is broadened and changed little with PIN incorporation in the composite. These results support that the fact that PIN and PIN/kaolinite composites are successfully synthesized.

Table 2 summarizes the TGA results of PIN and PIN/kaolinite composites. The PIN and PIN/kaolinite composites were degraded at one stage. The initial degradation temperatures of all the composites were observed to be higher than PIN. As the content of PIN was increased in the composite, the amount of residue left decreased. Tunney and Detellier studied the thermal behavior of kaolinite and they reported 650−800°C as degradation temperature, 730°C as half-life temperature and 88% of residue (17). Since, the thermal instability of ER active materials is an important problem to overcome, these thermal stability results of composites are very important for potential industrial applications of ER fluids.

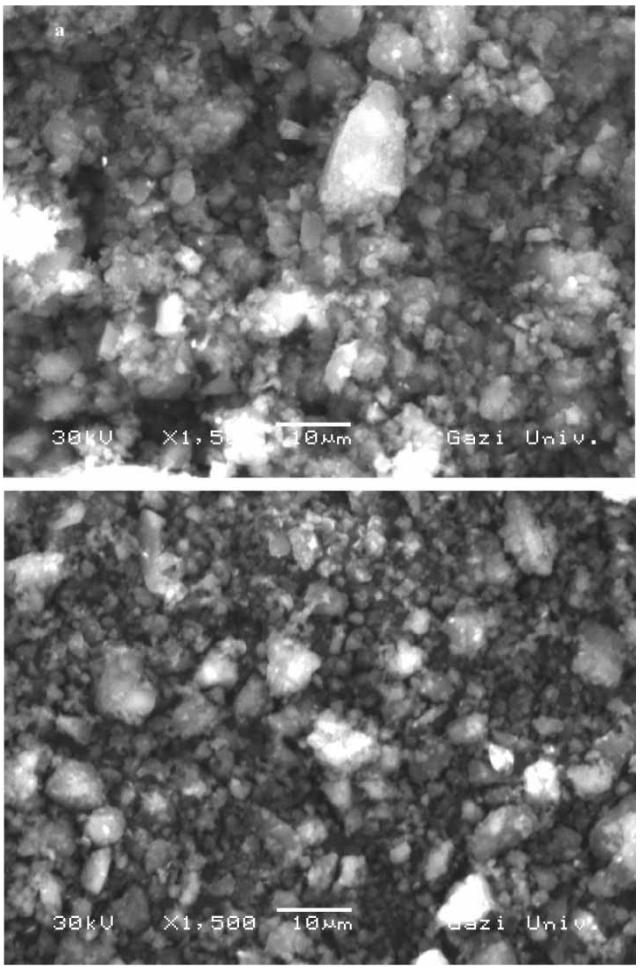

Fig. 2. SEM micrographs of (a) PIN and (b) PIN/kaolinite (K3) composite.

Figure 2 shows the SEM micrographs of PIN (a) and PIN/kaolinite (b) composites. Surface structure of both PIN and PIN/kaolinite (K3) composites were granular and porous; and their surface morphologies were similar to each other. Thus, it was concluded that, PIN and kaolinite formed harmonious and homogenous mixture in the composites (22).

Table 2. TGA Results of PIN and PIN/kaolinite composites

Sample	T_i (°C)	T_m (°C)	T_f (°C)	$T_{d(1/2)}$ (°C)	Residue (wt%) at 800°C
PIN	315	490	660	627	50
K1	385	490	595	516	72
K2	356	482	570	608	66
K3	335	471	570	625	37
K4	335	500	590	656	28
K5	340	515	606	685	25

T_i: Initial degradation temperature.
T_m: Maximum degradation temperature.
T_f: Final degradation temperature.
$T_{d(1/2)}$: Half life temperature.

3.2 Electrorheology

3.2.1 Effect of Concentration on ER Efficiency

Suspension concentration exerts a principle effect on the ER activity. The changes in ER efficiency, $((\eta_E - \eta_0)/\eta_0)$, with suspension concentrations of dispersed particles at constant shear rate ($\dot{\gamma} = 1.0\ s^{-1}$) and temperature ($T = 25°C$) are depicted in Figure 3. The ER efficiency increases with rising particle concentration up to c = 15 (m/m, %). This trend is due to the polarization forces acting between the suspended particles. The magnitude of this polarization force (F) in the direction of applied electric field (E) is (23).

$$F = 6\varepsilon_2 \cdot r^6 \cdot E^2/\rho^4 \quad (2)$$

Where ε_2 is the dielectric constant of the particle; ρ is the distance between particles, r is the radius of a particle.

Gradual decreases were observed at the ER efficiency of suspensions after c = 15 (m/m, %) particle concentration. As the amount of dispersed particles increased, η_0 also increased, which means that viscous forces dominated the suspension against electric field induced polarization forces.

Maximum ER efficiency of PIN and PIN/kaolinite composites/SO suspensions were observed to be: PIN (30.4) > K5 (29.3) > K4 (28.5) > K3 (26.5) > K2 (24.2) > K1 (20.6). The ER efficiencies of the composites were observed to increase with increasing PIN content.

Similar trends were reported in the literature by Langelova, Kordonsky and See for the ER studies of polyaniline/SO, cellulose derivatives/SO and poly(styrene-co-divinylbenzene)/SO suspensions, respectively (24, 25, 26).

3.2.2 Effect of Electric Field Strength on Viscosity

Figure 4 shows the change in the electric field viscosity (η_E) with electric field strength at constant conditions [$\dot{\gamma} = 1.0\ s^{-1}$, c = 15 (m/m, %), $T = 25°C$]. As seen from the graph, η_E of the suspensions increase slightly up to $E = 1.0$ kV/mm, then shows a sharp rise with enhanced electric field strength. Under an applied electric field strength, the magnitude of the interparticle interactions increases, and in turn, increases the chain length (formed by the polarized particles), resulting in the enhancement of in viscosity. Maximum η_E of the samples, under $E = 3.0$ kV/mm, were determined to be: PIN ($\eta_E = 908$ Pas) > K5 ($\eta_E = 798$ Pas) > K4 ($\eta_E = 746$ Pas) > K3 ($\eta_E = 698$ Pas) > K2 ($\eta_E = 332$ Pas) > K1 ($\eta_E = 271$ Pas). It was observed that, η_E of the composites increased with increasing PIN content.

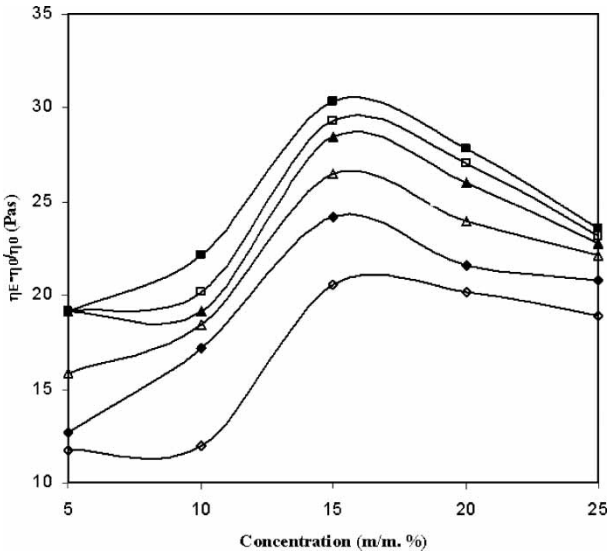

Fig. 3. Change in ER efficiency with concentration (■) PIN, (□) K5, (▲) K4, (△) K3, (◆) K2, (◇) K1, E = 0 kV/mm and E = 2.0 kV/mm, $\dot{\gamma} = 1.0\ s^{-1}$, $T = 25°C$.

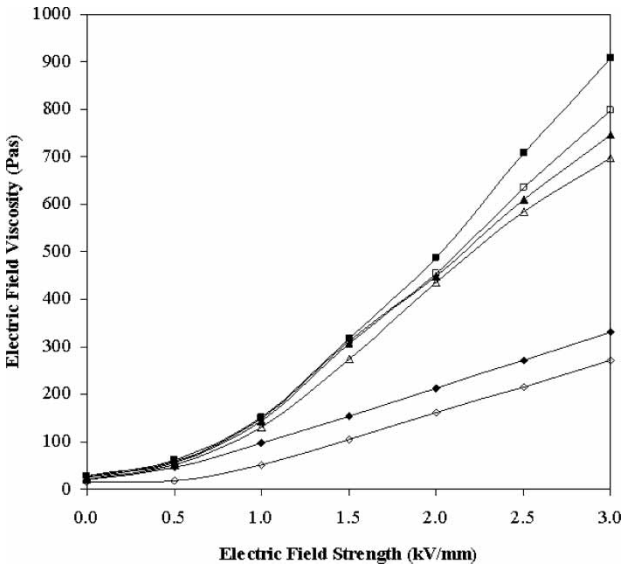

Fig. 4. The change of viscosity with electric field strength, (■) PIN, (□) K5, (▲) K4, (△) K3, (◆) K2, (◇) K1, c = 15 (m/m, %), $\dot{\gamma} = 1.0\ s^{-1}$, $T = 25°C$.

A similar trend of electric field viscosity change with external electric field strength was reported by Dürrschmith and Hoffmann (27) in ER studies of saponite/SO suspensions and by Unal et al. (28) in the ER studies of poly(Li-2-hydroxy ethyl methacrylate)/SO suspensions.

3.2.3 Effect of Electric Field Strength and Concentration on Shear Stress

Figure 5 shows the change in the yield stress ($\log\tau_y$) as a function of square of external electric field strength ($\log E^2$), keeping the shear rate ($\dot{\gamma} = 1.0\ s^{-1}$), suspension concentration (c = 15 (m/m, %), and temperature ($T = 25°C$) constant. It was determined that, for all the samples examined, τ_y increases with increasing E^2 and PIN content, indicating that the system structure in ER suspension become more stable under a strong electric field. When particles are subjected to an external electric field, their electric field-induced dipole moments increases proportionally and a stronger chain formation occurs between the suspended particles, which is in accordance with theoretical

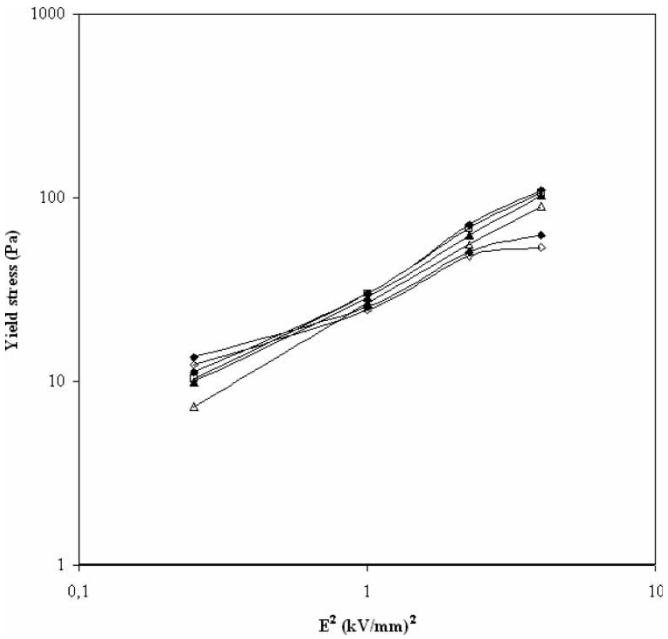

Fig. 5. Dependence of yield stress on electric field strength, (■) PIN, (□) K5, (▲) K4, (△) K3, (◆) K2, (◇) K1, c = 15 (m/m, %), $\dot{\gamma} = 1.0\ s^{-1}$, T = 25°C.

expectations:

$$\tau \propto E^n \tag{3}$$

This conclusion was confirmed in many other studies, i.e., glycerol-activated titania/SO (29), zeolite/SO (30), K_2O doped Y_2O_3/SO (31), β-cyclodextrin polymer/SO (32), and polyaniline/clay nanocomposites/SO (33) suspensions. Also, from the slope of $\log\tau_y$ vs. $\log E^2$, it was calculated that the slopes (m) were $m < 2$ (up to $E = 1$ kV/mm, $m = 0.42$; after $E = 1$ kV/mm, $m = 1.77$), which supports the proposed polarization model for ER active fluids by Choi (34).

In Figure 6, the change in electric field induced shear stress (τ_E) with concentration is given at constant conditions ($E = 2.0$ kV/mm, $\dot{\gamma} = 1.0\ s^{-1}$ and T = 25°C). The τ_E of an ER suspension is largely dependent on particle concentration. The following relationship is derived from Figure 6 (28):

$$\tau_E \propto c^{n(E)} \tag{4}$$

Electric field induced shear stress (τ_E) was observed to increase linearly with increasing suspended particle concentration and the PIN content of the composites. This is due to the increased magnitude of polarization forces at higher suspension concentrations, which results with enhanced τ_E. The change of τ_E of PIN and PIN/kaolinite/SO suspensions were as follows: τ_EPIN (285 Pa) > τ_EK5 (168 Pa)> τ_EK4 (123 Pa) > τ_EK3 (85 Pa) > τ_EK2 (70 Pa)> τ_EK1 (55 Pa). Kim (35) and Yavuz (36) reported similar trends for cellulose and poly(Li-tert-butylmethacrylate) suspensions prepared in SO, respectively.

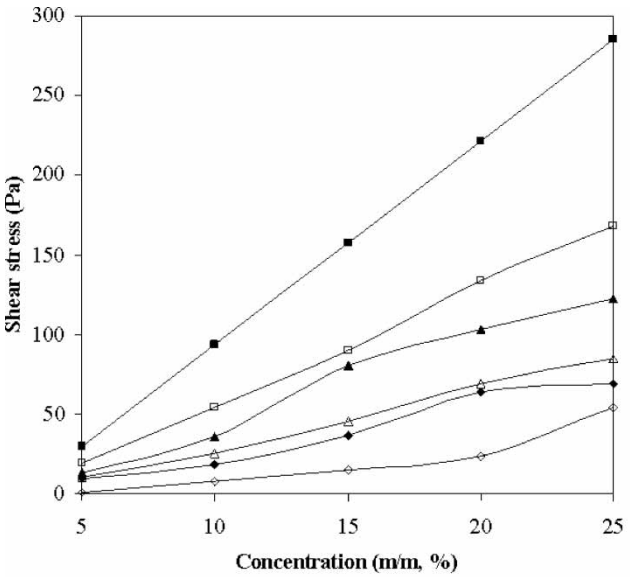

Fig. 6. The change of shear stress with concentration, (■) PIN, (□) K5, (▲) K4, (△) K3, (◆) K2, (◇) K1, E = 2 kV/mm, $\dot{\gamma} = 1.0\ s^{-1}$, T = 25°C.

3.2.4 *Effect of Shear Rate on Shear Stress*

Variation of shear stress for PIN and PIN/kaolinite composite suspensions in SO with shear rate at constant conditions (c = 15 m/m%., E = 2.0 kV/mm, T = 25°C) is shown in Figure 7. Shear stress increases with increasing shear rate as a typical of Bingham flow behavior. This is caused by the role of induced polarization forces, which is a typical rheological characteristic of ER fluids under the influence of external electric field strength (35).

Similar Bingham behavior was reported by Di et al., (37) for the ER studies of copper phthalocyanine-doped mesoporous TiO_2/SO suspensions.

3.2.5 *Effect of Shear Rate on Viscosity*

Change of viscosity of PIN and PIN/kaolinite composite suspensions in SO with shear rate/E^2 at constant conditions (c = 15 m/m%., E = 2.0 kV/mm, T = 25°C) is shown in Figure 8. Electric field viscosity of all the suspensions decreases sharply at smaller share rates, where the shear viscosity scales as:

$$\eta_E \propto \tau_E/\dot{\gamma} \tag{5}$$

At higher shear rates, the dependence of η_E become shear independent. This is a typical shear thinning non-Newtonian flow behavior of PIN and PIN/kaolinite composite/SO suspensions. Rheological properties of suspensions dramatically change upon the application of external electric field, which cause the rapid aggregation of particles into fibrous columns perpendicular to the parallel plate electrodes. These fibrous structures span the plate's gap in quiescent suspension and collapse with the increased shear rate. PIN and PIN/kaolinite composite particles are also affected by the

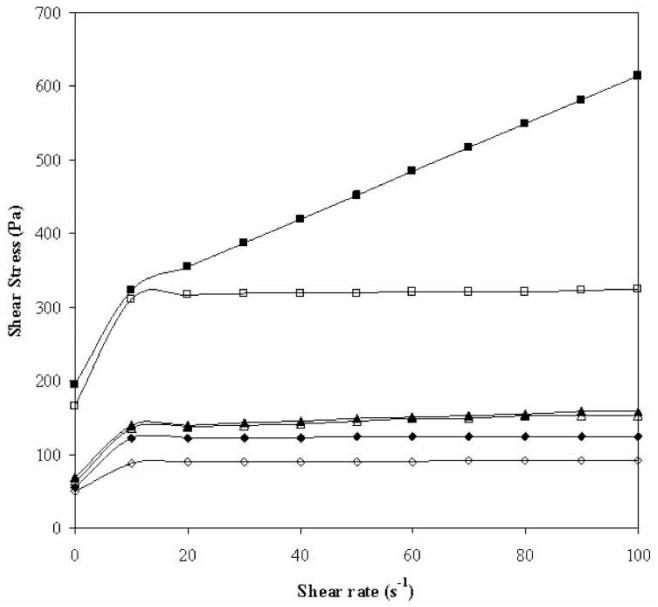

Fig. 7. The changes in shear stress with shear rate, (■) PIN, (□) K5, (▲) K4, (△) K3, (◆) K2, (◇) K1, c = 15 (m/m, %), E = 2 kV/mm, T = 25°C.

hydrodynamic interactions and the viscous forces (F) at high shear rates, which have the following magnitude (24):

$$F = 6\pi\eta_E r^2\dot{\gamma} \quad (6)$$

where, r is radius of particle. Although F is proportional to $\dot{\gamma}$, at higher shear rates, the suspension's viscosities become less dependent of on E. This suggests that at higher shear rates, the viscous forces are dominant over the polarization forces, and the suspensions structures do not vary appreciably with E. Similar behaviors were reported for poly(lithium-2-acrylamido-2-methyl propane sulfonic acid) (38), sepiolite (39), poly(naphtalene quinone) radical (40), cellulose (41), and PANI (42, 43), in all of which SO was used as the continuous phase for the suspensions.

3.2.6 *Effect of Frequency on ER Activity*

The external stress frequency (f) is an essential factor for characterizing the dynamic visco-elastic properties of ER fluids (44). Figure 9 demonstrates the change of electric field induced complex shear modulus (G') with f at c = 15%, E = 2.0 kV/mm and T = 25°C constant conditions. The setting shear stress for this experiment was $\tau = 10$ Pa, which can ensure that the measurements are conducted in the small strain region. The increase in G' with increasing external frequency was also reported in the literature (40, 45, 46) as the typical characteristic of a viscoelastic material.

3.2.7 *Effect of Temperature*

Figure 10 shows the changes in τ_E of PIN and PIN/kaolinite composite/SO suspensions under various temperatures at constant conditions (c = 15 m/m%, E = 2.0 kV/mm, $\dot{\gamma} = 1.0\ s^{-1}$). As the temperature increased from T = 0°C to T = 125°C, τ_E of all the suspensions were observed to decrease slightly. The shear stress losses [$\Delta\tau = \tau_{E(T=0°C)} - \tau_{E(T=125°C)}$] calculated from the graph were as follows: PIN ($\Delta\tau_E = 101$ Pa) > K3 ($\Delta\tau_E = 63$ Pa) > K5 ($\Delta\tau_E = 61$ Pa) > K4 ($\Delta\tau_E = 55$ Pa) > K2 ($\Delta\tau_E = 35$ Pa) > K1 ($\Delta\tau_E = 14$ Pa).

Generally, the temperature has two effects on the ER fluids: one is on polarization forces and another one is on the

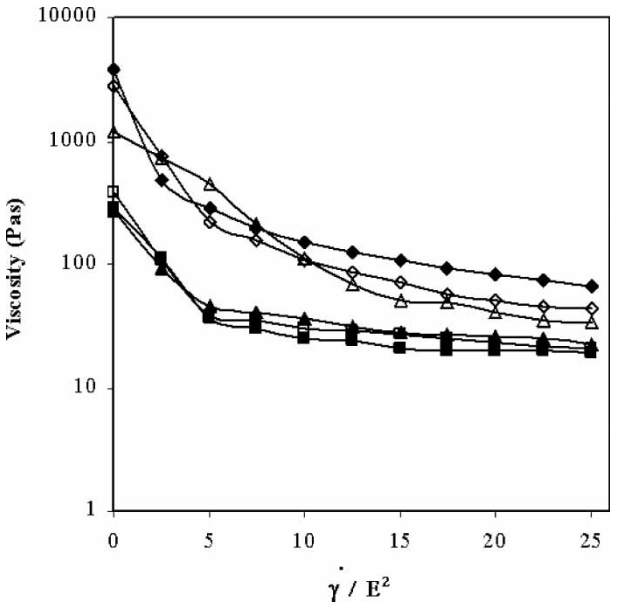

Fig. 8. The changes in viscosity with shear rate. (■) PIN, (□) K5, (▲) K4, (△) K3, (◆) K2, (◇) K1, c = 15(m/m), E = 2 kV/mm, T = 25°C.

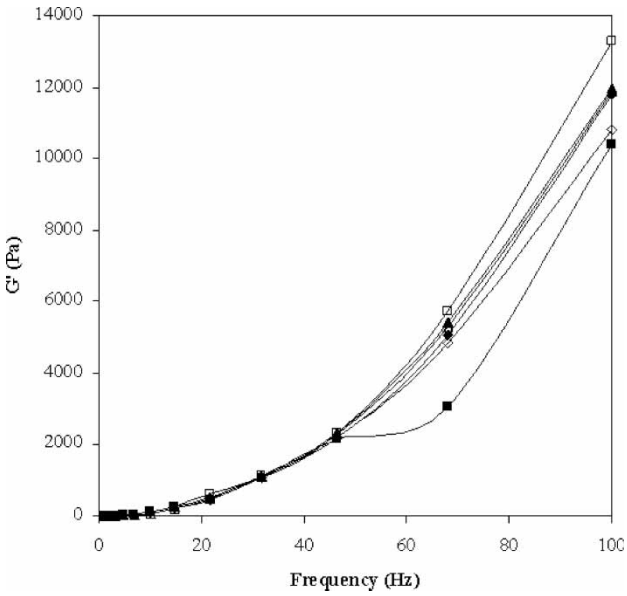

Fig. 9. The changes in elastic modulus with frequency (■) PIN, (□) K5, (▲) K4, (△) K3, (◆) K2, (◇) K1, c = 15 (m/m, %), E = 2.0 kV/mm, T = 25°C.

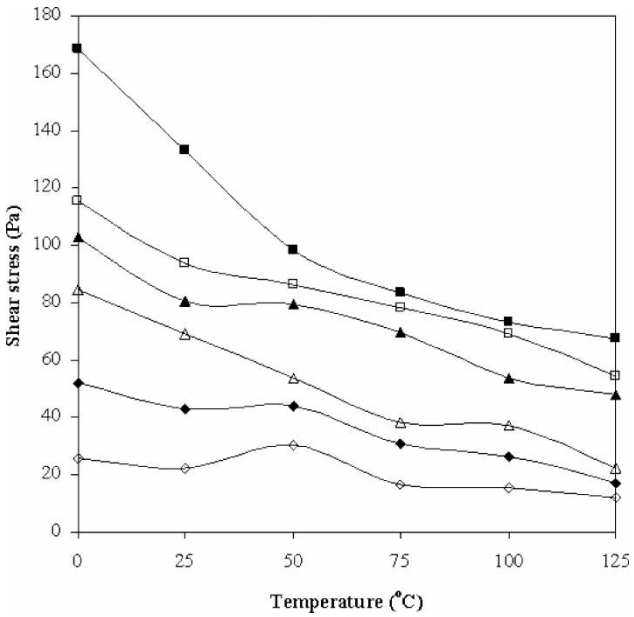

Fig. 10. The changes in shear stress with temperature, (■) PIN, (□) K5, (▲) K4, (△) K3, (◆) K2, (◇) K1, c = 15(m/m, %), E = 2.0 kV/mm, $\dot{\gamma} = 1.0\ s^{-1}$.

Brownian motion. The increase of temperature results both in decreased activation energy of polarization of suspended particles, and on the polarizability of particles, which results in a decrease in $\Delta\tau_E$. On the other hand, the Brownian motion does not contribute to chain formation of suspended particles. Although shear stress increases with increasing temperature reported in the literature by Choi (47) and Lu (48); Unal (29) and Liu (49) reported that shear stress decreases with increasing temperature.

The effects of promoter on the ER activity of PIN/kaolinite suspensions in SO were also investigated and it was observed that addition of any promoter (water, ethanol, glycerol) caused an electrical brake-down and caused no positive ER increment. That is why; the PIN and PIN/kaolinite suspensions examined in this study were classified as dry base ER fluids, which is an important property from an industrial point of view.

4 Conclusions

ER activity of all the suspensions was observed to increase with increasing electric field strength, concentration and decreasing shear rate.

The electric field viscosity of all the suspensions was decreased sharply with increasing shear rate, thus showing a typical shear thinning non-Newtonian visco-elastic behavior.

ER activity of suspensions increased with increasing PIN content in PIN/kaolinite composites.

Complex shear modulus of PIN and PIN/kaolinite suspensions was observed to increase with increasing external frequency and showing a typical characteristic of a visco-elastic material.

The ER strength of all the PIN and PIN/kaolinite suspensions was observed to be sensitive to high temperature, non-sensitive to promoter, and they were classified as dry base ER fluids and suitable for potential industrial applications.

5 Acknowledgments

This work was supported by the State Planning Organization of Turkey, (Grant No: 2001 K 120580) and Gazi University Research Fund (Grant No: FEF 05/2006-45). Special thanks to Dr. Metin GÜRÜ for SEM and TGA measurements.

6 References

1. Winslow, W.M. (1949) *J. Appl. Phys.*, **20**, 1137.
2. Hasley, T.C. (1992) *Science*, **258**, 761.
3. Choi, S.B., Choi, Y.T., Chang, E.G., Han, S.J. and Kim, C.S. (1988) *Mechatronics*, **8**, 14.
4. Alvin, P., Bradley, R., and Govindsami, T. (2006) EU patent no: WO2006057704.
5. Cho, M.S., Choi, H.J., Chin, I.J. and Ahn, W.S. (1999) *Micropor. Mesopor. Mater.*, **32**, 233.
6. Gehin, C., Persello, J., Charruat, D. and Cabane, B. (2004) *J. Coll. and Inter. Sci.*, **273**, 658.
7. Choi, U. (1999) *Coll. Surf A: Physicochem. Eng. Asp.*, **157**, 193.
8. Kim, S.G., Choi, H.J. and Jhon, M.S. (2001) *Macromol. Chem. Phys.*, **202**, 521.
9. Kim, J.W., Choi, H.J., Yoon, S.H. and Jhon, M.S. (2001) *Inter. Modern Phys. B*, **15**, 634.
10. Sohn, J.I., Sung, J.H., Choi, H.J. and Jhon, M.S. (2002) *J. Mater. Sci.*, **37**, 4057.
11. Parthasarathy, M. and Klingenberg, D.J. (1996) *Mat. Sci. Eng.*, **R17**, 57.
12. Zukoski, C.F. (1993) *Ann. Rev. Mat. Sci.*, **23**, 45.
13. Unal, H.I. and Yilmaz, H.J. (2002) *Appl. Polym. Sci.*, **86**, 1106.
14. Kawasumi, M., Hasegawa, N., Koto, M., Usuki, A. and Okada, A. (1997) *Macromolecules*, **30**, 6333.
15. Ogata, N., Kawakage, S. and Ogihara, T. (1997) *Polymer*, **38**, 5115.
16. Wang, Y. , Gao, J., Ma, Y. and Agarwal, U.S. (2006) *Composites Part B: Eng.*, **37**(**6**), 399.
17. Tunney, J.J. and Detellier, C. (1996) *Chem. Mater.*, **8**, 927.
18. German, R.M. In *Powder Metallurgy Science: Material Powder Industries Seperation*; Princeton, 28, 1994.
19. Chwang, C.P., Liu, C.D., Huang, S.W., Chao, D.Y. and Lee, S.N. (2003) *Synthetic Metals*, **142**(**1**–**3**), 275.
20. Kennedy, J.P., Midha, S. and Keszler, B. (1993) *Macromolecules*, **26**, 424.
21. Hahn, S.F. and Hillmyer, M.A. (2003) *Macromolecules*, **36**, 7.
22. Gök, A., Sarı, B. and Talu, M. (2003) *J. Appl. Polym. Sci.*, **89**, 2823.
23. Wu, S. and Shen, J. (1996) *J. Appl. Polym. Sci.*, **60**, 2159.
24. Langelova, A., Pavlinek, V., Saha, P., Quadrat, O., Kitano, T. and Stejskal, J. (2003) *Europan Polymer Journal*, **39**, 641.
25. Kordonsky, V.I., Korobko, E.V. and Larazeva, T.G. (1991) *J. Rheol.*, **35**, 1427.
26. See, H., Kawai, A. and Ikazaki, F. (2002) *Rheol. Acta*, **41**, 55.
27. Dürrschmidth, T. and Hoffmann, H. (1999) *Coll and Surf A: Physicochem Eng. Asp.*, **156**, 257.

28. Unal, H.I., Agirbas, O. and Yilmaz, H. (2006) *Coll. and Surf. A: Physicochem. Eng. Asp.*, **274**, 77.
29. Yin, J.B. and Zhao, X.P. (2003) *J. Coll. Inter. Sci.*, **257**, 228.
30. Tian, Y., Meng, Y. and When, S. (2001) *Materials Lett.*, **50**, 120.
31. Ni, N., Shang, Y.L., Li, J.R., Wang, J., Zhang, Y.J. and Zhang, S.H. (2006) *J. Alloys and Compounds*, **418**, 63.
32. Gao, Z. and Zhao, X. (2002) *Materials Lett.*, **57**, 615.
33. Lim, Y.T., Park, J.H. and Park, O.O. (2002) *J. Coll. Inter. Sci.*, **245**, 198.
34. Choi, H.J., Cho, M.S., Kim, J.W., Kim, C.A. and Jhon, M.S. (2001) *App. Physics Lett.*, **78**, 3806.
35. Kim, S.G., Kim, J.W., Jong, W.H., Choi, H.J. and Jhon, M.S. (2001) *Polymer*, **42**, 5005.
36. Yavuz, M. and Unal, H.I. (2004) *Turk. J. Chem.*, **28**, 587.
37. Di, K., Zhu, Y., Yang, X. and Li, C. (2006) *J. Coll. Inter. Sci.*, **294**, 499.
38. Unal, H.I. and Yilmaz, H. (2002) *J. App. Polym. Sci.*, **86**, 1107.
39. Unal, H.I., Yavuz, M. and Yilmaz, H. (2001) *Gazi Univ. J. Sci.*, **14**, 999.
40. Choi, H.J. and Cho, M.S. (2000) *Korea-Australia Rheology J.*, **12**, 151.
41. Choi, U. and Ahn, B. (2000) *Colloids and Surfaces A: Physicochem. Eng. Asp.*, **168**, 71.
42. Choi, H.J., Park, S.J., Kim, S.T. and Jhon, M.S. (2005) *Diamond Rel. Mat.*, **14**, 766.
43. Woo, D.J., Suh, M.H., Shin, E.S., Lee, C.W. and Lee, S.H. (2005) *J. Coll. Inter. Sci.*, **288**, 71.
44. Chin, B.D., Lee, Y.S. and Park, O.O. (1998) *Coll. Surf. A: Physicochem. Eng. Asp.*, **156**, 257.
45. Kim, J.W., Kim, S.G., Choi, H.J., Suh, M.S., Shin, M.J. and Jhon, M.S. (2001) *Int. J. Modern Phys. B*, **15**(**6**–**7**), 657.
46. Hiamtup, P., Sirivat, A. and Jameison, A.M. (2006) *J. Coll. Inter. Sci.*, **295**, 270.
47. Choi, U.S. (1999) *Coll. Surf. A: Physcochem. Eng. Asp.*, **157**, 192.
48. Lu, J. and Zhao, X. (2002) *International Modern Physics B*, **16**(**17**–**18**), 2521.
49. Liu, B. and Shaw, M.T. (2001) *J. Rheol.*, **45**, 641.